

Kinetics and Products of the Reactions of F2 with Br-Atom and Br2

Yuri Bedjanian, Manolis Romanias

▶ **To cite this version:**

Yuri Bedjanian, Manolis Romanias. Kinetics and Products of the Reactions of F2 with Br-Atom and Br2. International Journal of Chemical Kinetics, 2018, 50 (6), pp.425-434. 10.1002/kin.21171 . hal-02118007

HAL Id: hal-02118007
https://hal.science/hal-02118007

Submitted on 14 Jan 2022

HAL is a multi-disciplinary open access archive for the deposit and dissemination of scientific research documents, whether they are published or not. The documents may come from teaching and research institutions in France or abroad, or from public or private research centers.

L'archive ouverte pluridisciplinaire **HAL**, est destinée au dépôt et à la diffusion de documents scientifiques de niveau recherche, publiés ou non, émanant des établissements d'enseignement et de recherche français ou étrangers, des laboratoires publics ou privés.

Kinetics and products of the reactions of F_2 with Br-atom and Br_2

YURI BEDJANIAN[*] and MANOLIS N. ROMANIAS[#]

ICARE, CNRS and Université d'Orléans, 45071 Orléans Cedex 2, France

ABSTRACT. Reactions of F_2 molecules exhibit unusual features, manifesting in high reactivity of F_2 with respect to some closed-shell molecules and low reactivity toward chemically active species, such as halogen and oxygen atoms. The existing data base on the reactions of F_2 being rather sparse, kinetic and mechanistic studies (preferably over a wide temperature range) are needed in order to better understand the nature of the specific reactivity of fluorine molecule. In the present work, reactions of F_2 with Br atoms and Br_2 have been studied for the first time in an extended temperature range using a discharge flow reactor combined with an electron impact ionization mass spectrometer. Rate constant of the reaction $F_2 + Br \rightarrow F + BrF$ (1) was determined either from kinetics of the reaction product, BrF, formation or from the kinetics of Br consumption in excess of F_2: $k_1 = (4.66 \pm 0.93) \times 10^{-11} \exp(-(4584 \pm 86)/T)$ $cm^3 molecule^{-1} s^{-1}$ at T= 300-940 K. The rate constant of the reaction $F_2 + Br_2 \rightarrow$ products (2), $k_2 = (9.23 \pm 2.68) \times 10^{-11} \exp(-(8373 \pm 194)/T)$ cm^3 $molecule^{-1}$ s^{-1}, was determined in the temperature range 500-958 K by monitoring both reaction product (FBr) formation and F_2 consumption kinetics in excess of Br_2. The results of the experimental measurements of the yield of FBr (1.02 ± 0.07 at T = 960K) combined with thermochemical calculations indicate that $F+Br_2F$ forming channel of the reaction (2) is probably the dominant one, at least, at highest temperature of the study.

Keywords: Fluorine, bromine, kinetics, rate coefficient, temperature dependence.

[*]*Correspondence to:* Yuri Bedjanian: Tel.: +33 238255474, e-mail: yuri.bedjanian@cnrs-orleans.fr.

[#] Now at IMT Lille Douai, SAGE, F-59508, Douai, France.

Supporting Information is available in the online issue at www.wileyonlinelibrary.com.

INTRODUCTION

Reactivity of F_2 molecules exhibits certain specific features and is an interesting case for kinetic studies. So, on the one hand, molecular fluorine manifests relatively high reactivity with respect to some closed-shell molecules and, on the other hand, it relatively slowly reacts with chemically active species, such as halogen and oxygen atoms. It was demonstrated, for example, that reactions of F_2 with organosulfur compounds, CH_3SCH_3 and CH_3SSCH_3, and with limonene are barrierless reactions [1-3]. Unexpectedly high (for reaction between two closed-shell molecules) value, 1.6×10^{-11} $cm^3molecule^{-1}s^{-1}$ at 298 K, was reported for the rate constant of the reaction of F_2 with CH_3SCH_3 [4]. At the same time, rate constants reported for reactions of F_2 with Cl, Br and O atoms are lower than 10^{-16} $cm^3molecule^{-1}s^{-1}$ at room temperature [5]. The existing data base on the reaction of F_2 is rather sparse [5] and more kinetic and mechanistic studies (preferably over a wide temperature range) are needed in order to better understand the nature of the specific reactivity of F_2 molecule.

In the present work we report the results of an experimental study of the reactions of molecular fluorine with Br_2 and Br-atoms in an extended temperature range (from room temperature to 958 K):

$Br + F_2$	$\rightarrow F + FBr$	$\Delta_rH° = -21.8$ kcal mol^{-1}	(1)
$Br_2 + F_2$	$\rightarrow FBr + FBr$	$\Delta_rH° = -35.5$ kcal mol^{-1}	(2a)
	$\rightarrow F + Br_2F$	unknown	(2b)
	$\rightarrow Br + F_2Br$	unknown	(2c)
	$\rightarrow FBr + F + Br$	$\Delta_rH° = 24.3$ kcal mol^{-1}	(2d)

The thermochemical data used for the calculations of $\Delta_rH°$ are from ref. 6. In addition to general interest, the information on these reactions is of practical interest for laboratory studies of chemical systems where bromine and fluorine are simultaneously present in their

molecular and/or atomic form. For example, Br_2 is frequently used (as in the present work) as a fluorine atom scavenger

$$F + Br_2 \rightarrow BrF + Br \quad (3)$$

in order to detect and/or measure the absolute concentrations of F-atoms [3,7,8].

Previously, rate constant of reaction (1) was determined twice, however, in a limited low temperature range: by Strattan and Kaufman [9] between 296 and 418K and by Arutyunov et al. [10] at T = 298K. To our knowledge, this is the first kinetic study of the reaction of F_2 with Br_2.

METHODS

Experimental

Experiments were carried out in a discharge flow reactor using a modulated molecular beam mass spectrometer with electron impact ionization as the detection method. The flow reactor operated at temperatures T = 300 – 960 K and nearly 2 Torr total pressure of Helium and consisted of an electrically heated Quartz tube (45 cm length and 2.4 cm i.d.) with water-cooled extremities (Fig. S1, Supporting Information) [11]. Temperature in the reactor was measured with a *K*-type thermocouple positioned in the middle of the reactor in contact with its outer surface. Temperature gradients along the flow tube measured with a thermocouple inserted in the reactor through the movable injector was found to be less than 1% [11].

Br atoms were formed in the microwave discharge of Br_2/He mixtures. It was verified by mass spectrometry that more than 95% of Br_2 was dissociated in the microwave discharge. Br atoms were detected directly at their parent peak m/z = 79/81 (Br^+) or as BrCl (m/z = 116) upon chemical conversion in reaction with an excess of ClNO (added in the end of the reactor 5 cm upstream of the sampling cone, see Fig. S1):

$$Br + ClNO \rightarrow BrCl + NO \quad (4)$$

Absolute concentrations of Br atoms were determined from the fraction of Br_2 dissociated in the microwave discharge: $[Br] = 2\Delta[Br_2]$. Bromine fluoride, BrF, observed as a product of reactions (1) and (2), was monitored at m/z = 98/100 (BrF^+). Mass spectrometric signals of BrF were absolutely calibrated using chemical conversion of F atoms to BrF in reaction (3) with excess Br_2. The absolute concentration of BrF was determined as $[BrF] = \Delta[Br_2]$, i.e. from the consumed fraction of $[Br_2]$. F atoms in the calibration experiments were formed in the microwave discharge of F_2/He mixtures. In order to reduce F atom reactions with Pyrex surface inside the microwave cavity, a ceramic (Al_2O_3) tube was inserted in this part of the injector. The absolute concentrations of Br_2 as well as of other stable species (F_2, ClNO) in the reactor were calculated from their flow rates obtained from the measurements of a pressure drop over time of their mixtures in He stored in calibrated volume reservoirs. It can be noted that both F_2 and Br_2 are thermally stable in the temperature range of the present study. We have not observed any experimental evidence for significant thermal decomposition of these species on the timescale of the present experiments, even at highest temperatures, in agreement with the existing kinetic data on their thermal stability [5]. In particular, we did not observe the formation of Br atoms that could be formed upon decomposition (homogeneous or heterogeneous) of Br_2 in the reactor.

It should be noted that due to technical difficulties related to the change in surface-to-volume ratio of the main reactor, we have not carried out specific test experiments in order to estimate the possible role of wall reactions in the present study. The possible contribution of the heterogeneous chemistry was assumed to be negligible and was not considered.

The purities of the gases used were as follows: He >99.9995% (Alphagaz), passed through liquid nitrogen trap; Br_2 >99.99% (Aldrich); F_2, 5% in helium (Alphagaz); ClNO > 97% (Matheson).

Computational methodology

Thermochemical calculations were carried out to determine the unknown enthalpies of reaction pathways (2b) and (2c). To that end, the Gaussian 09 program suite was used [12]. The strategy applied to determine the thermochemical parameters was as follows: various methods and standard basis sets were deployed to perform electronic structure calculations, geometry optimizations and vibrational frequency calculations for the reaction pathways with known reaction enthalpy, (2a) and (2d). Then, the method/basis set combinations that provided reaction enthalpies close to the known $\Delta_r H°$ of reactions (2a) and (2d) were selected for calculations of the enthalpies of the reaction pathways (2b) and (2c). Further improvement of electronic and thermal enthalpies calculated has been achieved by applying spin–orbit coupling corrections. Density functional theory (B3LYP, BHandHLYP) and Moller plesset perturbation (MP2), were the methods tested. These methods were combined with the following standard basis sets: 6-31G(d) (valence double zeta and polarization functions on heavy atoms), 6-311G(d) (valence triple zeta and polarization on heavy atoms), AUG-CC-PVDZ (valence double zeta, polarization and diffuse) and CC-PVTZ (valence triple zeta and polarization on all atoms). Overall B3LYP was the best performer among the tested methods, and its combination with 6-31G(d), 6-311G(d) and CC-PVTZ provided the most accurate results based on the selection criteria discussed above. In case of 6-31G(d), extra single point calculations were performed by applying the composite G3B3 method. More precisely, this compound method consisted of geometry optimization and vibrational frequency calculations at the B3LYP/6-31G(d) level and then a series of single-point energy calculations at four different higher levels of theory QCISD(T)/6-31G(d), MP4/6-31+G(d), MP4/6-31G(2df,p), and MP2/G3Large were performed to the optimized structure. Finally the average values of $\Delta_r H°$ obtained within G3B3 and B3LYP/ CC-PVTZ methods were used to estimate the thermodynamic parameters of the reactions (2b) and (2c).

RESULTS AND DISCUSSION

Rate constant of reaction (1)

The rate constant of reaction Br+ F_2 was determined using two different methods. In the first one, used at lower temperatures, where reaction (1) is relatively slow and consumption of the reactants is too low to be measured accurately, the rate constant was determined by monitoring the kinetics of the reaction product, BrF. The second approach, a common one, used at higher temperatures (T = 755 and 940 K), consisted in a direct monitoring of the kinetics of Br-atom consumption in excess of F_2.

Kinetics of BrF production in reaction (1). In this series of experiments, the rate constant of reaction (1) was determined in the temperature range 300 - 770 K from the kinetics of the reaction product, BrF, formation under conditions where consumption of reactants (Br and F_2) was negligible (less than 5 % at all temperatures of the study). Under conditions where concentration of Br and F_2 are constant, the BrF formation is governed by zeroth order kinetics, $d[BrF]/dt = k_1 \times [Br] \times [F_2]$ = const, and linear increase of the product concentration with reaction time is expected. Experiments were carried out in the presence of Br_2 in the reactor ($[Br_2] = (0.6\text{-}2.2) \times 10^{13}$ molecule cm^{-3}), which led to a rapid conversion of the second product of reaction (1), fluorine atom, to BrF through reaction (3) ($k_3 = (1.28 \pm 0.2) \times 10^{-10}$ $cm^3 molecule^{-1} s^{-1}$ at T = 299 -940K) [7]. Thereby, the kinetics of BrF formation corresponded to the following equation:

$$d[FBr]/dt = 2k_1 \times [Br] \times [F_2] \qquad (I)$$

Examples of the kinetics of BrF production are shown in Fig. 1. The slopes of the straight lines in Fig. 1 provide the rate of BrF production, d[BrF]/d*t* (in molecule $cm^{-3} s^{-1}$). The rate of BrF production measured as a function of product of the concentrations of Br and F_2 at different temperatures is shown in Figs. 2 and S2-S3 (Supporting Information).

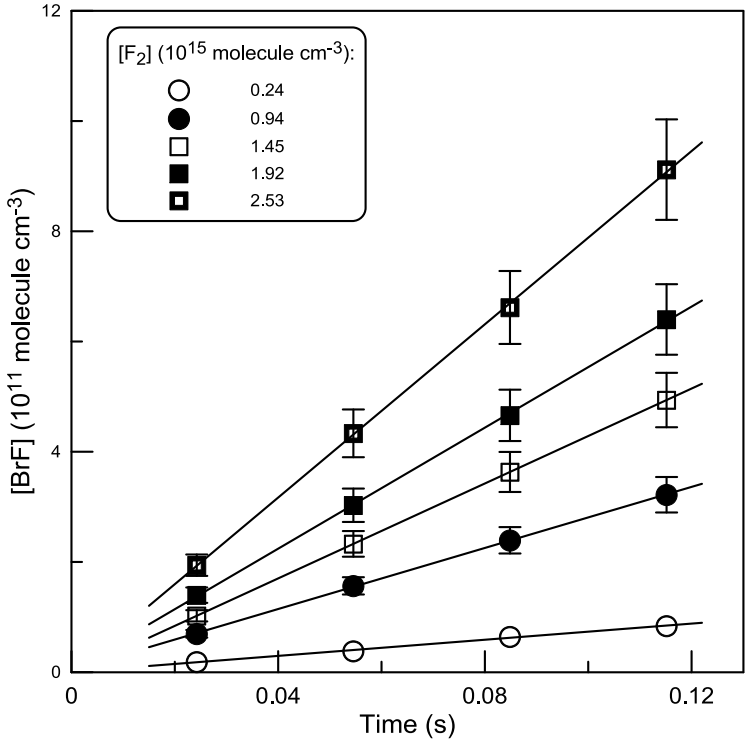


Figure 1 Reaction Br + F_2: kinetics of BrF production measured at T = 315 K with [Br] ≈ 7×10^{13} molecule cm^{-3} and different initial concentrations of F_2. Error bars represent maximum uncertainty of 10% on determination of [BrF]. Continuous lines represent linear fit to the experimental data.

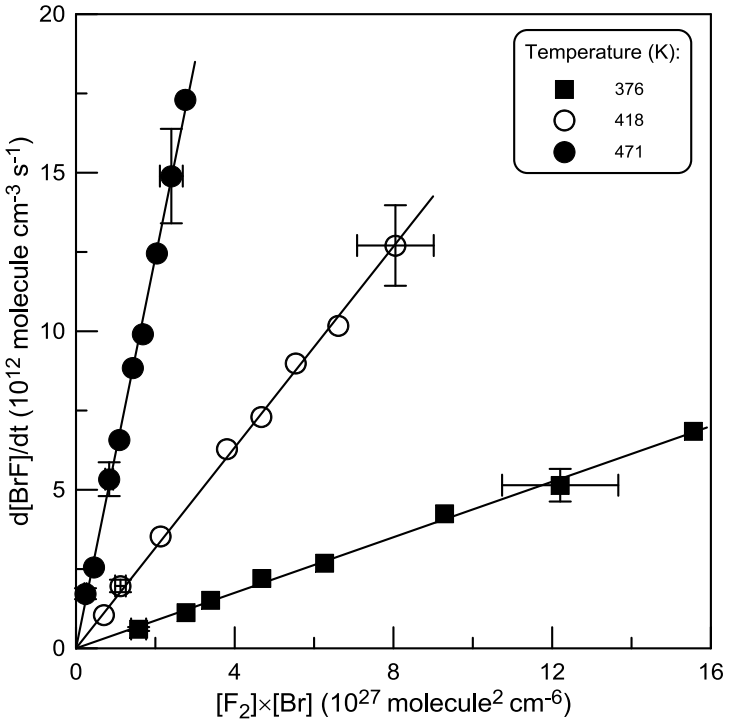


Figure 2 Reaction Br + F_2: examples of the dependence of the rate of BrF production on the product of the concentrations of Br and F_2. Error bars represent typical uncertainties on the determination of d[FBr]/d*t* and $[F_2]\times[Br]$, nearly 10 and 12 %, respectively.

The slopes of the observed linear dependences of d[FBr]/dt on [F_2]×[Br] provide, in accordance with equation (I), the values of $2\times k_1$ at respective temperatures. All the data obtained in this way for the rate constant of reaction (1), as well as initial concentrations of the reactants used in these experiments, are shown in Table I. The combined uncertainty on the measurements of k_1 was estimated to be of nearly 20%, by adding in quadrature (square root of the sum of squares) the statistical error ($\leq$ 7%) and those on the measurements of the flows (5%), pressure (2%), temperature (1%) and absolute concentrations (~10%) of the three species involved.

It can be noted that in the measurements of k_1, the possible secondary reaction (-3) (endothermic by 13.7 kcal mol^{-1}) [6]:

$$Br + FBr \leftrightarrows F + Br_2 \qquad (-3, 3)$$

is not expected to impact the temporal profiles of FBr, the equilibrium (-3, 3) being shifted to the left under the experimental conditions of the study. The contribution of the reaction

$$Br_2 + F_2 \rightarrow \text{products} \qquad (2)$$

to the side production of FBr was observed (with microwave discharge off, i.e. in the absence of Br atoms in the reactive system) to be negligible and was estimated (using k_2 measured in the present study) to be less than 1.4% at T = 770 K, highest temperature of the measurements.

Table I Reaction Br + F_2: Experimental Conditions and Results of the Measurements of the Rate Constant

T (K)	number of kinetic runs	[Br]^a	[F_2]^b	$k_1{}^c$	method
300	9	81.6-105	2.31-30.7	0.0111	FBr kinetics
315	8	67.9-77.8	2.36-25.3	0.0197	FBr kinetics
343	8	16.7-18.4	3.41-20.2	0.0810	FBr kinetics
376	8	9.55-11.0	1.48-15.9	0.219	FBr kinetics
418	8	8.96-9.74	0.756-8.36	0.790	FBr kinetics
471	8	11.0-13.1	0.218-2.17	3.08	FBr kinetics
539	9	1.71-2.27	0.226-3.53	10.6	FBr kinetics

638	7	1.98-3.02	0.131-2.58	30.9	FBr kinetics
755	8	≤ 0.6	0.698-11.3	107	Br kinetics
770	10	3.44-4.79	0.088-0.533	138	FBr kinetics
940	9	≤ 0.3	0.690-8.38	315	Br kinetics

[a] Unit is 10^{12} molecule cm^{-3}.
[b] Unit is 10^{14} molecule cm^{-3}.
[c] Unit is 10^{-15} $cm^3 molecule^{-1} s^{-1}$; statistical 1σ and estimated systematic uncertainties on k_1 are (3-7) % and ≈20%, respectively.

Kinetics of Br-atom consumption in excess of F_2. Reaction of Br atoms with F_2 is relatively slow; for this reason the experiments on the determination of k_1 from Br decays were conducted at two temperatures, T = 755 and 940K, at high temperature limit of the temperature range used. The initial concentrations of Br atoms and F_2 used in these experiments are shown in Table I. Two methods were used for monitoring Br atoms. In experiments at T = 755 K, ClNO (~ 3×10^{13} molecule cm^{-3}) was added at the end of the reactor 5 cm upstream of the sampling cone of the mass spectrometer and Br atoms were converted to BrCl via reaction (4) and detected at m/z = 116 ($BrCl^+$). At T = 940K, Br atoms were monitored at their parent peak at m/z = 79/81 (Br^+), corrected for the contribution of the reaction product, FBr, at this mass due to its fragmentation in the ion source of the mass spectrometer. Examples of the exponential Br-atom decays are shown in Fig. S4 (Supporting Information). Consumption of F_2 was negligible in all experiments due to its high excess over Br atoms. Figure 3 demonstrates the pseudo-first order rate constants, $k_1' = k_1[F_2] + k_w$, measured as a function of the concentration of F_2. k_w represents the rate of Br-atom decay in the absence of F_2 in the reactor and was measured in separate experiments ($k_w \leq 3$ s^{-1}). All measured values of k_1' were corrected for axial and radial diffusion [13] of bromine atoms. The corrections on k_1' were calculated using diffusion coefficient of Br in He, $D_0 = 480 \times (T/298)^{1.75}$ Torr cm^{-2} s^{-1} (estimated with Fuller's method) [14] and were less than 20 %. The slopes of the straight lines in Fig. 3 provide the values of k_1 at T = 755 and 940K, shown in Table I. It should be noted that the possible reproduction of Br atoms in a rapid secondary

reaction (3) of F atoms with Br_2 was insignificant under experimental conditions of the study due to very low concentration of Br_2. In fact, Br_2 was observed to be completely dissociated in the microwave discharge. In addition, in order to reduce the heterogeneous recombination of Br atoms upon their transport to the main reactor and considering that surface recombination of Br atoms is inhibited by molecular fluorine [9,10] small amount of F_2 (~10^{12} molecule cm^{-3}) was added in the movable injector. As a result, the concentration of Br_2 in the main reactor was measured to be < 10^{10} molecule cm^{-3}.

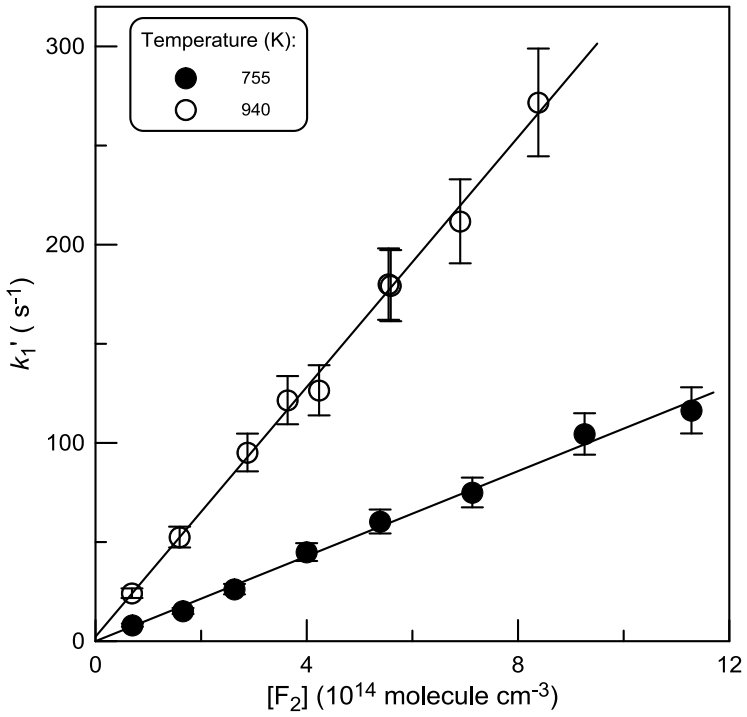


Figure 3 Reaction Br + F_2: pseudo-first order plots obtained from Br-atom decay kinetics in excess of F_2. Error bars represent maximum uncertainty of 10% on determination of k_1'.

All the results obtained for k_1 at different temperatures of the study are shown in Fig. 4. The unweighted exponential fit to the present data for k_1 (solid black line) yields the following Arrhenius expression:

$k_1 = (4.66 \pm 0.93) \times 10^{-11} \exp(-(4584 \pm 86)/T)$ $cm^3 molecule^{-1} s^{-1}$,

where the cited uncertainties are 2σ statistical ones.

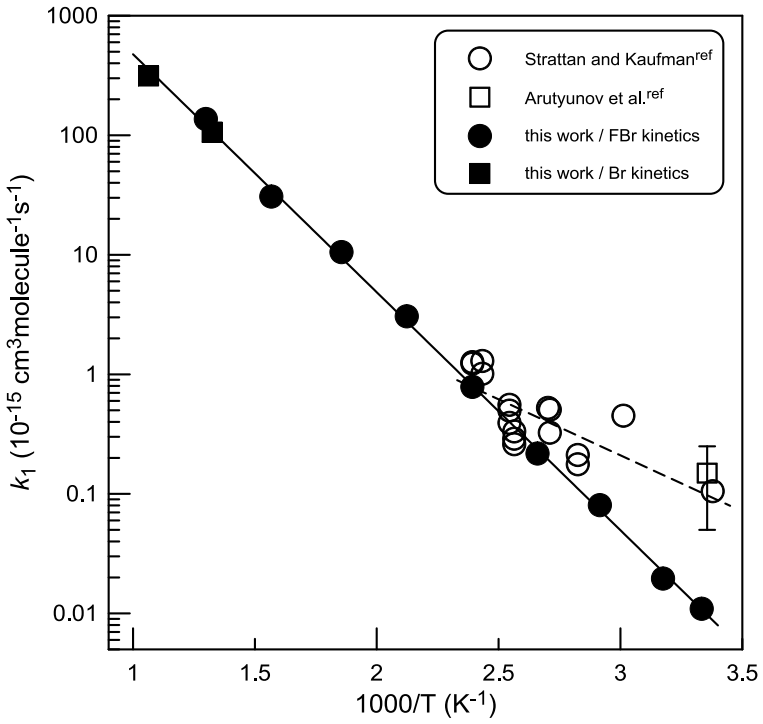


Figure 4 Reaction Br + F_2: summary of the experimental data for the reaction rate constant. Uncertainty on the values of k_1 from the present study (nearly 20%) corresponds to the size of the symbols.

Reaction F_2 + Br_2

Reaction thermochemistry. Reaction of F_2 with Br_2 can proceed through four different channels. The enthalpies of the reaction pathways (2a) and (2d) can be calculated from the tabulated enthalpies of formation of the species involved [6]. The unknown enthalpies of the reactions (2b) and (2c) were calculated in the present work (Table II) following the approach described in section II.B. The calculations revealed that for the reaction pathways (2a) and (2d), the thermochemical data obtained with B3LYP/CC-PVTZ and G3B3 methods were almost identical to corresponding values derived from the known enthalpies of formation. Consequently, these methods were chosen to estimate the enthalpies of the channels (2b) and (2c) leading to the following thermochemical data for reactions 2a to 2d (Table II):

Table II Reaction $F_2 + Br_2$: Thermochemical Data Calculated Using Different Methods and Standard Basis Sets

reaction channel	$\Delta_r H°$ (kcal mol^{-1})									
	MP2/		BHandHLYP/			B3LYP/			average[a]	from $\Delta_f H°$[b]
	AUG-CC-PVDZ	6-311G(d)	6-31G(d)	6-311G(d)	CC-PVTZ	6-311G(d)	CC-PVTZ	G3B3		
2a	-45.7	-29.3	-31.2	-30.7	-36.7	-29.8	-35.5	-35.5	-35.5	-35.5
2b	12.6	19.5	22.7	8.3	8.8	14.3	13.8	20.6	17.2	unknown
2c	18.1	22.8	28.8	12.8	13.8	28.3	28.8	25.8	27.3	unknown
2d	19.9	24.5	30.9	13.8	10.6	29.2	25.4	23.3	24.4	24.3

[a] Average thermal energy values calculated using the B3LYP/ CC-PVTZ and G3B3 methods.
[b] Calculated from the tabulated enthalpies of formation of the species involved in the reactions [6].

$Br_2 + F_2 \rightarrow FBr + FBr$ $\Delta_r H° = -35.5$ (-35.5) kcal mol^{-1} (2a)

$\rightarrow F + Br_2F$ $\Delta_r H° = (13.8 – 20.6)$ kcal mol^{-1} (2b)

$\rightarrow Br + F_2Br$ $\Delta_r H° = (25.8 – 28.8)$ kcal mol^{-1} (2c)

$\rightarrow FBr + F + Br$ $\Delta_r H° = 24.4$ (24.3) kcal mol^{-1} (2d)

(for reactions (2a) and (2d), the values in parenthesis are those calculated using thermochemical data from ref. 6; all enthalpies are given at T = 298K).

Kinetics of BrF production in reaction (2). The rate constant of the reaction Br_2+ F_2 was determined from the kinetics of the reaction product, BrF, at T = 500-945 K and kinetics of F_2 consumption in excess of Br_2 at highest temperature of the study, T = 958 K. The kinetics of BrF formation was monitored under conditions where consumption of the reactants (Br_2 and F_2) was negligible (< 10%). As one could expect, a linear increase of product concentration with reaction time was observed (Fig. 5).

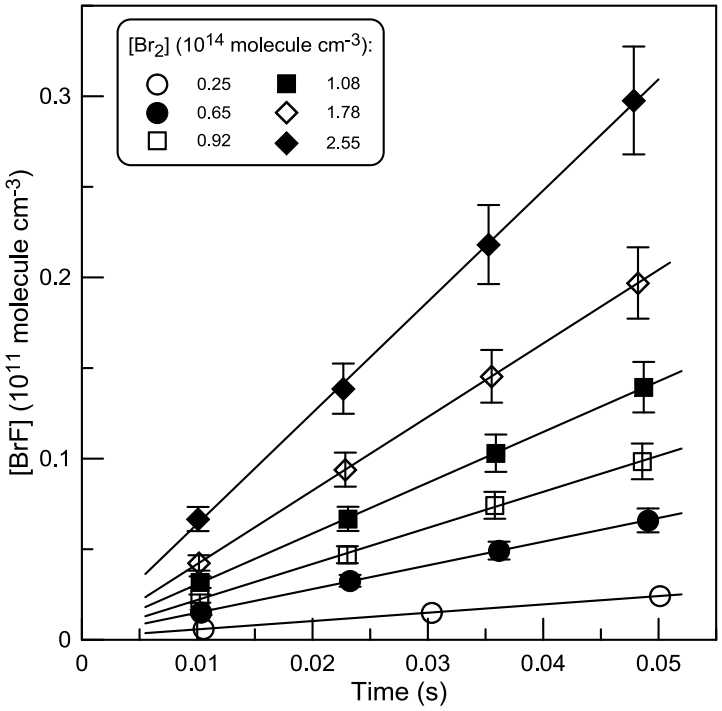


Figure 5 Reaction Br_2 + F_2: kinetics of BrF production measured at T = 664K with $[F_2] \approx 7.5\times10^{13}$ molecule cm^{-3} and different initial concentrations of Br_2. Error bars represent maximum uncertainty of 10% on determination of [BrF]. Continuous lines represent linear fit to the experimental data.

In the temperature range used and considering the reaction activation energy of (16.6 ± 0.4) kcal mol^{-1} determined in the present study (see below), reaction channels (2c) and (2d) can be ruled out as too endothermic. Two reaction channels, (2a) and (2b), lead to BrF formation in the chemical system used: directly, in reaction (2a) and through rapid conversion of fluorine atom, formed in reaction (2b), to BrF via reaction F+Br_2. Thereby, the observed kinetics of BrF formation correspond to the following equation:

$$d[BrF]/dt = (2k_{2a} + k_{2b}) \times [Br_2] \times [F_2] \quad \text{(II)}$$

The slopes of the straight lines in Fig. 5 provide the rate of BrF production, d[BrF]/d*t* (in molecule $cm^{-3}s^{-1}$). The rate of BrF production measured as a function of product of the concentrations of Br_2 and F_2 at different temperatures is shown in Figs. 6 and S5-S6 (Supporting Information).

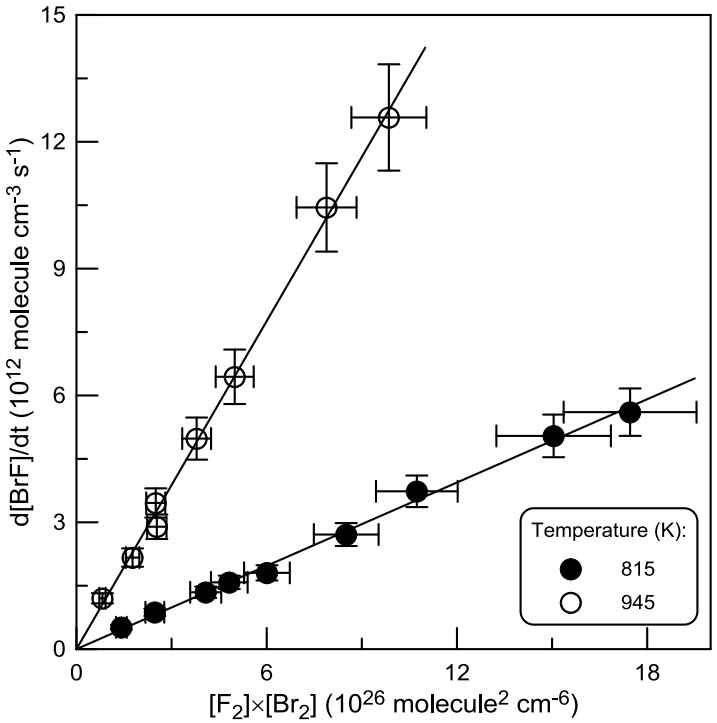


Figure 6 Reaction Br_2 + F_2: examples of the dependence of the rate of BrF production on the product of the concentrations of Br_2 and F_2. Error bars represent typical uncertainties on the determination of d[FBr]/d*t* and $[F_2]\times[Br_2]$, nearly 10 and 12 %, respectively.

The slopes of the observed linear dependences of d[FBr]/dt on $[F_2]\times[Br_2]$ provide, in accordance with equation (II), the values of $2k_{2a} + k_{2b}$ at respective temperatures. All the data obtained in this way are shown in Table III.

Table III Reaction $F_2 + Br_2$: Experimental Conditions and Results of the Measurements of the Rate Constant

T (K)	Number of kinetic runs	$[Br_2]^a$	$[F_2]^b$	rate constant^c	method
500	9	39.1-251	6.0-68.1	0.0437	BrF kinetics
545	10	3.70-23.8	36.4-40.7	0.222	BrF kinetics
624	10	1.56-23.9	6.61-8.03	1.50	BrF kinetics
664	9	2.50-25.6	6.70-8.09	2.89	BrF kinetics
714	10	1.23-19.0	3.31-3.52	6.93	BrF kinetics
815	9	1.26-18.3	0.95-1.35	32.8	BrF kinetics
945	8	1.25-15.3	0.61-0.66	129	BrF kinetics
958	8	40.0-401	≈ 0.2	152	F_2 kinetics

[a] Unit is 10^{13} molecule cm^{-3}.
[b] Unit is 10^{13} molecule cm^{-3}.
[c] Corresponds to $2k_{2a} + k_{2b}$ (BrF kinetics) and k_2 (total rate constant, F_2 kinetics); unit is 10^{-16} $cm^3 molecule^{-1} s^{-1}$; statistical 1σ uncertainties are in the range(5-9) %; estimated combined uncertainties on k_2 determined from BrF and F_2 kinetics are 25 and 20%, respectively.

It should be noted that Br atoms, formed upon conversion of F to BrF in reaction (3), are present in the reactive system and can lead to additional production of BrF in reaction (1):

$$Br_2 + F_2 \rightarrow F + Br_2F \qquad (2b)$$

$$F + Br_2 \rightarrow BrF + Br \qquad (3)$$

$$Br + F_2 \rightarrow F + BrF \qquad (1)$$

The extent of this secondary BrF production was estimated using the rate constants of the reactions (1), (2) and concentrations of Br_2 and Br ([Br] ≈ [BrF]) and was found to be insignificant in most experiments due to high $[Br_2]$ to [Br] ratios under the experimental conditions of the measurements. Corrections on the contribution of reaction (1) applied to the measured rate of BrF formation generally ranged from a few to 20%, however reached up to a factor of 1.6 under certain experimental conditions at lower temperatures. The combined

uncertainty on the measurements of k_2 in these experiments was estimated to be of nearly 25 %, including statistical error (≤ 9%) and those on the measurements of the flows (5%), pressure (2%), temperature (1%), absolute concentrations (~10%) of the three species involved and applied corrections.

Kinetics of F_2 consumption in excess of Br_2. Reaction $Br_2 + F_2$ being very slow, the experiments on the determination of k_2 from F_2 decays were conducted only at highest temperature of the study, T = 958 K. The initial concentrations of the reactants, Br_2 and F_2, used in these experiments are shown in Table III. Examples of the exponential decays of F_2 are presented in Fig. S7. Figure 7 demonstrates the pseudo-first order rate constants, $k_2' = k_2[Br_2]$, measured as a function of concentration of Br_2.

All the measured values of k_2' were corrected for axial and radial diffusion [13] of F_2. The corrections on k_2' were calculated using diffusion coefficient of F_2 in He, $D_0 = 427 \times (T/298)^{1.75}$ Torr cm^{-2} s^{-1} (estimated with Fuller's method) [14] and were in the range (3-30) %. Consumption of F_2 in secondary reaction (1) with Br atoms was insignificant (estimated to be < 10% under experimental conditions used) due to sufficient excess of Br_2 over F_2 and was not taken into account. The slope of the straight line in Fig. 7 yields the value of $k_2 = (1.52 \pm 0.30)\times10^{-14}$ $cm^3molecule^{-1}s^{-1}$ at T = 958K (with 20% estimated uncertainty). This value corresponding to the total rate constant of reaction (2), $k_2 = k_{2a} + k_{2b}$, is in good agreement with that measured for $2k_{2a} + k_{2b}$ from kinetics of BrF production at T = 945K.

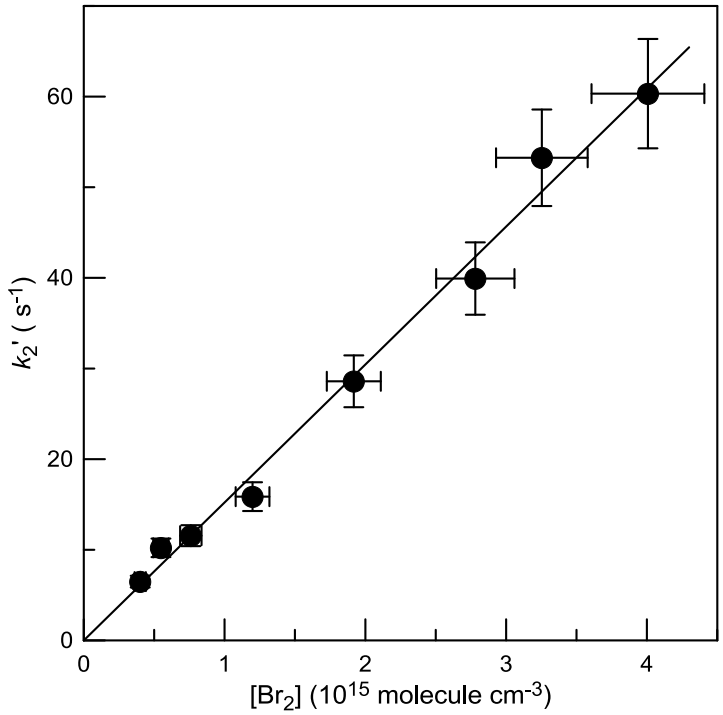


Figure 7 Reaction $Br_2 + F_2$: pseudo-first order plot obtained from F_2 decay kinetics in excess of Br_2 at T = 958K. Error bars correspond to nearly 10% uncertainties on the determination of k_2' and [Br_2].

All the results obtained for k_2 at different temperatures are shown in Fig. 8. The unweighted exponential fit to the present data for k_2 (solid black line) yields the following Arrhenius expression:

$k_2 = (9.23 \pm 2.68) \times 10^{-11} \exp(-(8373 \pm 194)/T)$ cm^3 molecule^{-1} s^{-1}

(cited uncertainties are 2σ statistical ones), showing that reaction (2) proceeds with an activation energy of (16.6 ± 0.4) kcal mol^{-1}.

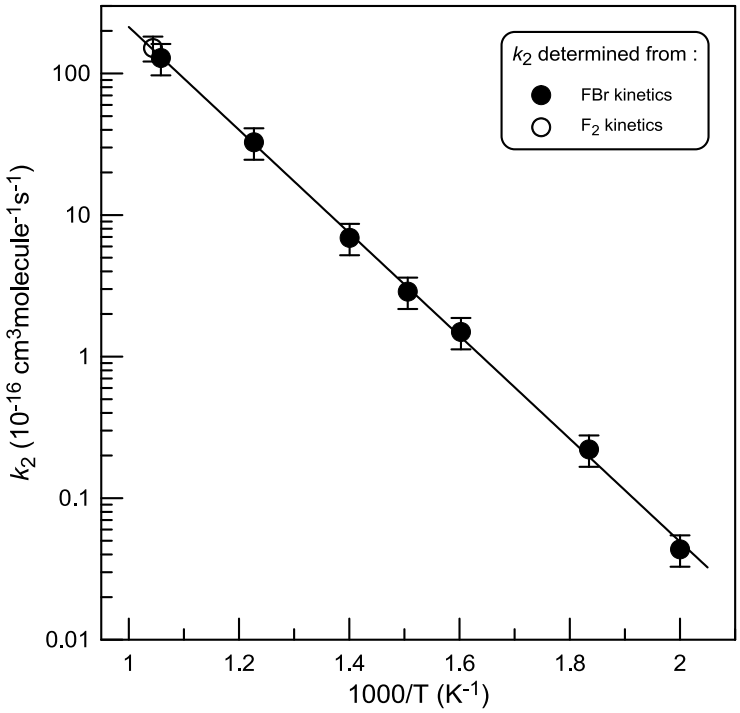


Figure 8 Reaction $Br_2 + F_2$: temperature dependence of the reaction rate constant. Error bars correspond to 25 and 20% uncertainty on the determination of k_2 from FBr and F_2 kinetics, respectively.

Yield of BrF in reaction (2). In these experiments, carried out at T = 960K, we have monitored the concentration of BrF formed as a function of the concentration of F_2 consumed in reaction with excess Br_2 ($[Br_2] \sim 10^{15}$ molecule cm^{-3}) at a fixed reaction time of nearly 0.05 s. Under these experimental conditions approximately half of the initial concentration of F_2 was consumed. The observed experimental data are shown in Fig. 9. The slope of the straight line in Fig. 9 corresponds to the number of FBr molecules (reaction (2a)) and F atoms (reaction (2b) followed by reaction (3)) formed per one F_2 molecule consumed in reaction with Br_2 and provides the branching ratio $(2k_{2a} + k_{2b})/k_2 = 1.02 \pm 0.07$ ($\pm 2\sigma$) at T = 960K. Under assumption of the negligible contribution of the channels (2c) and (2d) (see above) and considering that (i) two BrF molecules are formed in reaction (2a) per one consumed molecule of F_2 and (ii) the experimental fact, that the measured ratio $(2[BrF]_{channel(2a)}+[F]_{channel(2b)})/\Delta[F_2]$ is close to one, it seems reasonable to suggest that F + Br_2F forming pathway of the reaction (2) is the dominant one, at least, at highest temperature

(T = 960K) of the present study. This is in line with the kinetic measurements showing an excellent agreement (see Fig. 8) between $2k_{2a} + k_{2b}$ derived from BrF kinetics and total rate constant, $k_2 = k_{2a} + k_{2b}$, measured from F_2 decays at highest temperature of the study. We failed to detect Br_2F by mass spectrometry at m/z =179 (Br_2F^+). The fate of this radical, if formed, is unknown. However, the results of the measurements of the yield of BrF indicate that possible reactions of Br_2F, at least, do not lead to BrF production in the reactive system and under the experimental conditions used, i.e. do not impact the results of the kinetic measurements.

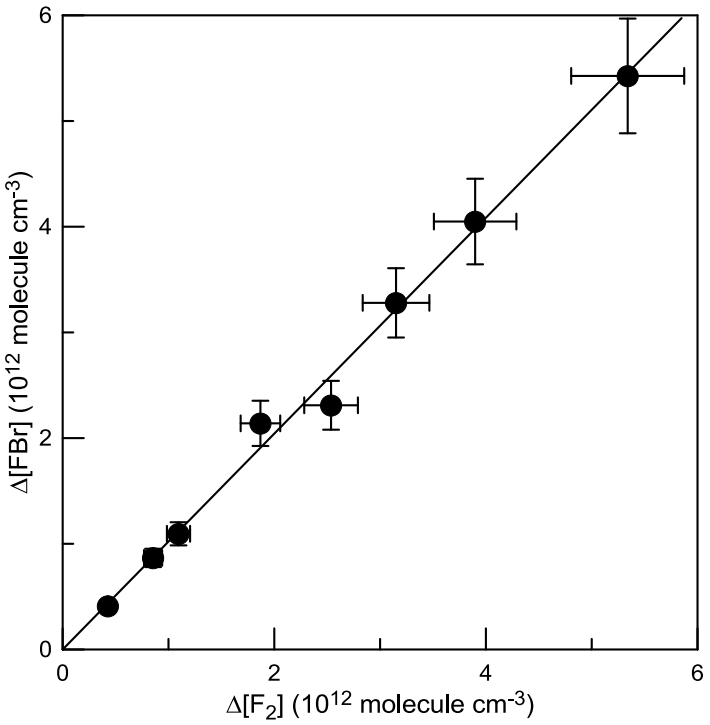


Figure 9 Reaction $Br_2 + F_2$: concentration of BrF formed as a function of the consumed concentration of F_2 at T = 960K. Error bars correspond to typical 10% uncertainties on the determination of the absolute concentrations of the relevant species. Continuous line represents linear through origin fit to the experimental data.

Comparison with previous data

To our knowledge, this is the first study of the reaction between Br_2 and F_2. The kinetics of the reaction of Br-atom with F_2 was explored in two previous studies [9,10]. Strattan and Kaufman [9] have determined the rate constant of reaction (1) over the temperature range

296-418 K in a flow reactor by monitoring BrF produced at fixed reaction time in a mixture of Br, Br_2 and F_2 (open circles in Fig. 4). The dashed line in Fig. 4 corresponds to the Arrhenius expression reported by the authors for k_1:

$k_1 = 1.31 \times 10^{-13} \exp(-2154/T)$ cm^3 molecule^{-1} s^{-1}

Arutyunov et al. [10] reported $k_1 = (1.5 \pm 1) \times 10^{-16}$ cm^3 molecule^{-1} s^{-1} at T = 298K, which was measured in a flow reactor combined with ESR detection of Br atoms. One can note that although the Arrhenius expression reported for k_1 by Strattan and Kaufman [9] significantly differs from that of the present work, the absolute values of the rate constant from two studies at T $\geq$ 350 K are in satisfactory agreement especially when considering within a factor of 2 accuracy on the individual rate constants reported in ref. 9. On contrary, the room temperature value of k_1 measured in the present work is by an order of magnitude lower compared with two previous measurements. The reasons for such a significant discrepancy can be numerous and they are difficult to establish, in particular, due to the absence of the experimental details in ref. 10, where the rate constant was determined from Br decays in excess of F_2 with high initial concentrations of Br (~10^{14} molecule cm^{-3}) and in presence of oxygen atoms ([Br]/[O]≈3.5). From general considerations, it is clear that measuring the rate constant of such a slow reaction from Br decays in a flow reactor at a total pressure of 0.2-4 Torr and a maximum contact time of 0.1s is rather delicate (low consumption of Br), especially, with low sensitivity of ESR spectrometer to Br atoms. Accordingly, and as noted by the authors, the reproducibility of the results was rather low. In the study of Strattan and Kaufman [9], where the reaction rate constant was determined by monitoring the reaction product BrF (like present study), the kinetics of BrF formation was found to be nonlinear and displaying acceleration of BrF production rate with time. To escape this problem, the authors applied an alternative method of determining k_1, which consisted in measuring of [BrF] produced at a fixed reaction time as a function of [F_2]. However, considering the curvature of BrF kinetics, it seems that

the value of the rate constant measured by this method could depend on the choice of the fixed reaction time (higher rate constant at longer reaction time).

The Arrhenius expression of k_1 determined in the present study shows that reaction of Br with F_2 is relatively slow (despite its exothermicity) due to significant (≈ 9.1 kcal mol^{-1}) activation energy. As discussed in previous studies [9,10], energetic barrier is expected for both transition state $[BrFF]^{\dagger}$ and $[FBrF]^{\dagger}$, which results from Br insertion between two fluorine atoms. In the first case, as suggested by Politzer [15], it is due to anomalously large repulsive forces (specific for F-atom because of its exceptionally small size) arising when an external electron enters outer shell of fluorine atom. In the second case, insertion of Br atom in F_2 molecule should require substantial energy needed for separation of two fluorine atoms, and an activation barrier equal to significant fraction of the F-F bond dissociation energy can be expected.

CONCLUSION

In this work, kinetics of the reactions of F_2 with Br-atom (reaction 1) and Br_2 (reaction 2) were investigated as a function of temperature at nearly 2 Torr total pressure of helium. The following Arrhenius expressions, $k_1 = (4.66 \pm 0.93) \times 10^{-11} \exp(-(4584 \pm 86)/T)$ and $k_2 = (9.23 \pm 2.68) \times 10^{-11} \exp(-(8373 \pm 194)/T)$ $cm^3 molecule^{-1} s^{-1}$, were determined for the rate coefficients of these reactions at T= 300-940 and 500-958 K, respectively. The results of the measurements of the yield FBr (1.02 ± 0.07 at T = 960K) in reaction (2) combined with thermochemical calculations suggest that $F+Br_2F$ forming channel of the reaction (2) is probably the dominant one, at least, at highest temperature of the study.

Financial support from CNRS is gratefully acknowledged.

BIBLIOGRAPHY

1. Lu, Y.-J.; Lee, L.; Pan, J.-W.; Xie, T.; Witek, H. A.; Lin, J. J. J. Chem. Phys. 2008, 128, 104317.
2. Shao, H.-C.; Xie, T.; Lu, Y.-J.; Chang, C.-H.; Pan, J.-W.; Lin, J. J. J. Chem. Phys. 2009, 130, 014301.
3. Bedjanian, Y.; Romanias, M. N.; Morin, J. J. Phys. Chem. A 2014, 118, 10233-10239.
4. Turnipseed, A. A.; Birks, J. W. J. Phys. Chem. 1991, 95, 6569-6574.
5. Manion, J. A.; Huie, R. E.; Levin, R. D.; Burgess, D. R.; Orkin, V. L.; Tsang, W.; McGivern, W. S.; Hudgens, J. W.; Knyazev, V. D.; Atkinson, D. B.; Chai, E.; Tereza, A. M.; Lin, C.-Y.; Allison, T. C.; Mallard, W. G.; Westley, F.; Herron, J. T.; Hampson, R. F.; Frizzell, D. H. NIST Chemical Kinetics Database, NIST Standard Reference Database 17, Version 7.0 (Web Version), Release 1.6.8, Data version 2015.12, National Institute of Standards and Technology, Gaithersburg, Maryland, 20899-8320; Vol. 2017. http://kinetics.nist.gov/ (accessed December 2017).
6. Burkholder, J. B.; Sander, S. P.; Abbatt, J.; Barker, J. R.; Huie, R. E.; Kolb, C. E.; Kurylo, M. J.; Orkin, V. L.; Wilmouth, D. M.; Wine, P. H. Chemical Kinetics and Photochemical Data for Use in Atmospheric Studies, Evaluation No. 18, JPL Publication 15-10, Jet Propulsion Laboratory; JPL Publication 15-10, Jet Propulsion Laboratory: Pasadena, 2015. http://jpldataeval.jpl.nasa.gov (accessed December 2017).
7. Bedjanian, Y. J. Phys. Chem. A 2017, 121, 8341-8347.
8. Bedjanian, Y.; Lelièvre, S.; Bras, G. L. J. Photochem. Photobio. A 2004, 168, 103-108.
9. Strattan, L. W.; Kaufman, M. J. Chem. Phys. 1977, 66, 4963-4967.
10. Arutyunov, V. S.; Buben, S. N.; Chaikin, A. M. Kinet. Catal. 1979, 20, 465-469.
11. Morin, J.; Romanias, M. N.; Bedjanian, Y. Int. J. Chem. Kinet. 2015, 47, 629-637.
12. Frisch, M. J.; Trucks, G. W.; Schlegel, H. B.; Scuseria, G. E.; Robb, M. A.; Cheeseman, J. R.; Scalmani, G.; Barone, V.; Mennucci, B.; Petersson, G. A.; Nakatsuji, H.; Caricato, M.; Li, X.; Hratchian, H. P.; Izmaylov, A. F.; Bloino, J.; Zheng, G.; Sonnenberg, J. L.; Hada, M.; Ehara, M.; Toyota, K.; Fukuda, R.; Hasegawa, J.; Ishida, M.; Nakajima, T.; Honda, Y.; Kitao, O.; Nakai, H.; Vreven, T.; Montgomery Jr., J. A.; Peralta, J. E.; Ogliaro, F.; Bearpark, M. J.; Heyd, J.; Brothers, E. N.; Kudin, K. N.; Staroverov, V. N.; Kobayashi, R.; Normand, J.; Raghavachari, K.; Rendell, A. P.; Burant, J. C.; Iyengar, S. S.; Tomasi, J.; Cossi, M.; Rega, N.; Millam, N. J.; Klene, M.; Knox, J. E.; Cross, J. B.; Bakken, V.; Adamo, C.; Jaramillo, J.; Gomperts, R.; Stratmann, R. E.; Yazyev, O.;

Austin, A. J.; Cammi, R.; Pomelli, C.; Ochterski, J. W.; Martin, R. L.; Morokuma, K.; Zakrzewski, V. G.; Voth, G. A.; Salvador, P.; Dannenberg, J. J.; Dapprich, S.; Daniels, A. D.; Farkas, Ö.; Foresman, J. B.; Ortiz, J. V.; Cioslowski, J.; Fox, D. J. Gaussian 09; Gaussian, Inc.: Wallingford, CT, USA, 2009.

13. Kaufman, F. J. Phys. Chem. 1984, 88, 4909-4917.
14. Tang, M. J.; Cox, R. A.; Kalberer, M. Atmos. Chem. Phys. 2014, 14, 9233-9247.
15. Politzer, P. J. Am. Chem. Soc. 1969, 91, 6235-6237.